Short-term forecasting of renewable production trajectories at high-temporal resolution

Simon Camal, Dennis Van Der Meer, George Kariniotakis MINES Paris - PSL University

25 May 2022 EGU 2022

This project has received funding from the European Union's Horizon 2020 research and innovation programme under grant agreement No 864337

- A forecast does not have value until it is used in some decision-making process.
- The combination of RES with battery storage requires high temporal resolution forecasts (≤ 5 min).
- Use Cases for power system management require different forecasting horizons, e.g. hour-ahead or day-ahead

Forecasting marginal CDFs and estimating a covariance matrix become cumbersome at very high resolution and/or large forecast horizons. For instance, 48 h at 5 min equals 576 marginals or 24 h at 1 min equals 1440 marginals.
We develop a high-temporal resolution intra-day and day-ahead model using pattern matching (PMM) that downscales NWP forecasts.

- PMM does not require training but only proper data organization;
- PMM is about 98% faster than the state-of-the-art; and
- PMM incurs only a minor performance penalty.

- The proposed pattern matching model (PMM) is based on the analog ensemble [ADSC15].
- Compare the entire horizon of the most recent NWP forecast ("query" $\mathcal{X}_t$) to historical NWP forecasts ("analogs" $\mathcal{A}$).
- Distance metric: $d(\mathcal{X}_t, \mathcal{A}_i) = \sqrt{\sum_{j=1}^{J} w_j^h \left(x_t^{(j)} - x_i^{(j)}\right)^2}$.
- Search by k-d tree: any type of input feature, 3 orders of magnitude faster than brute-force search [Yv21].
- Best trajectory: $\boldsymbol{f}_s = \begin{pmatrix} y_{i+1} & \cdots & y_{i+12\cdot K} \end{pmatrix} \odot \begin{pmatrix} G^{cs}_{t+1} & \cdots & G^{cs}_{t+12\cdot K} \end{pmatrix}$.

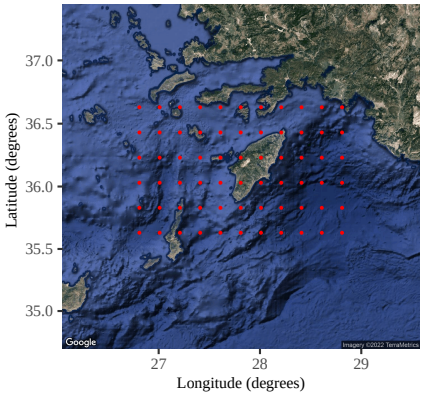

Figure 1: Overview of the NWP grid points around Rhodes, Greece.

Input features:

- Total PV power of Rhodes, Greece (18 MW), detrended using McClear clear-sky model [LOB$^+$13]);
- Processed ECMWF NWP ensembles: Mean and st.dev. of members at each grid point (MS) / Quantiles over all ensemble members and grid points (QS);
- Solar zenith angle.

Setup:

- Hourly forecast updates
- One year of available data $\rightarrow$ circular testing on one month

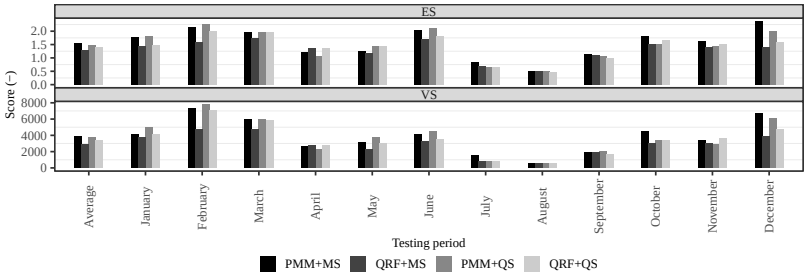

Figure 2: ES and VS averaged over the entire testing set and on a monthly basis. Scores are dimensionless.

Some observations:

- QRF+MS performs best overall but limited testing size $\rightarrow$ block bootstrapped confidence intervals of forecast error loss differential $d_t = \ell(\boldsymbol{F}_{1,t}, \boldsymbol{y}_t) - \ell(\boldsymbol{F}_{2,t}, \boldsymbol{y}_t)$;
- $H_0 : \mathbb{E}(\boldsymbol{d}) = 0$ and $H_a : \mathbb{E}(\boldsymbol{d}) \neq 0$, $\alpha = 5\% \rightarrow$ Fail to reject H_0.

- We proposed a forecast model based on pattern matching to generate trajectories at any temporal resolution (limited by available data);
- The statistical test does not allow to conclude on significant difference in performance between the proposed model and the state-of-the-art
- Perspective: evaluate value in power system application (eg storage)
- The proposed model was about 98% faster and does not require training;
- Would most likely benefit from more historical data.

[ADSC15] S. Alessandrini, L. Delle Monache, S. Sperati, and G. Cervone.
An analog ensemble for short-term probabilistic solar power forecast.
Applied Energy, 157:95–110, 2015.

[LOB+13] M. Lefèvre, A. Oumbe, P. Blanc, B. Espinar, B. Gschwind, Z. Qu, L. Wald, M. Schroedter-Homscheidt, C. Hoyer-Klick, A. Arola, A. Benedetti, J. W. Kaiser, and J.-J. Morcrette.
McClear: a new model estimating downwelling solar radiation at ground level in clear-sky conditions.
Atmospheric Measurement Techniques, 6(9):2403–2418, 2013.

[Yv21] Dazhi Yang and Dennis van der Meer.
Post-processing in solar forecasting: Ten overarching thinking tools.
Renewable and Sustainable Energy Reviews, 140:110735, 2021.

Thanks!

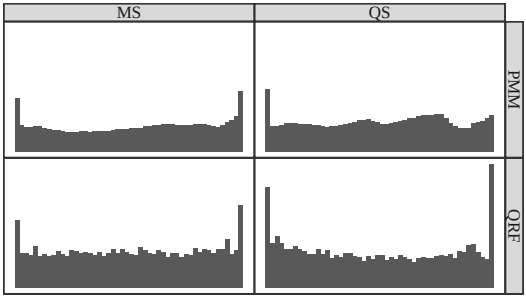

Figure 3: Histograms of the marginal PIT variables combined over all forecast horizons and testing instances where the zenith angle is lower than 85°.

Some observations:

- PMM+MS and QRF+QS forecasts tend to be underdispersed;
- QRF+MS and PMM+QS are better calibrated in the main distribution except for deviation in the extreme quantiles.

Table 1: Block bootstrapped loss differential presented as $\mu \pm \sigma$ (2.5% – 97.5%).

	ES			
	PMM+QS	QRF+QS	PMM+MS	QRF+MS
PMM+QRF	0±0 (0—0)	0.06±0.31 (-0.5—0.83)	-0.08±0.21 (-0.67—0.31)	0.13±0.32 (-0.4—0.82)
QRF+QS	(-)	0±0 (0—0)	-0.11±0.29 (-0.78—0.46)	0.11±0.22 (-0.2—0.68)
PMM+MS	(-)	(-)	0±0 (0—0)	0.15±0.27 (-0.31—0.74)
QRF+MS	(-)	(-)	(-)	0±0 (0—0)
	VS			
	PMM+QS	QRF+QS	PMM+MS	QRF+MS
PMM+QS	0±0 (0—0)	397.02±1116.4 (-1557.52—3187.29)	-246.11±794.92 (-1996.46—1632.91)	722.43±1199.35 (-977.84—3611.67)
QRF+QS	(-)	0±0 (0—0)	-533.09±1108.93 (-3073.65—1598.25)	534.45±1119.49 (-657.42—4011.29)
PMM+MS	(-)	(-)	0±0 (0—0)	776.92±1091.41 (-770.52—3274.18)
QRF+MS	(-)	(-)	(-)	0±0 (0—0)

- We fail to reject $H_0 : \mathbb{E}(\boldsymbol{d}) = 0$.

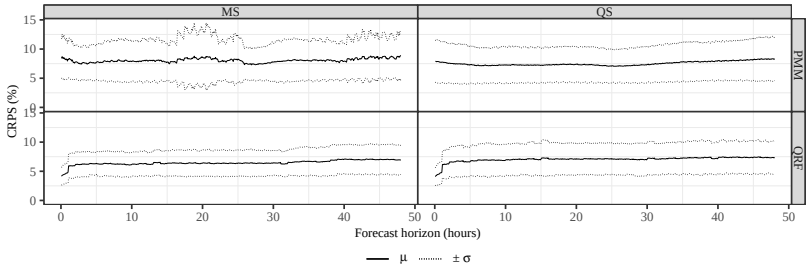

Figure 4: CRPS in percent of nominal capacity as a function of forecast horizon. The mean and standard deviation are computed across the 12 testing months.

Some observations:

- CRPS of PMM+QS is constant over the forecast horizon, whereas CRPS of QRF+MS and QRF+QS increases sharply over the first hours and then stabilizes;
- QRF performs best but more data would likely benefit PMM more than QRF.